Subgrid modeling in particle-laden channel flow

Subgrid modeling in particle-laden channel flow

J. G. M. Kuerten[a)]
Department of Mechanical Engineering, J.M. Burgers Center, Technische Universiteit Eindhoven, P.O. Box 513, 5600 MB Eindhoven, The Netherlands

(Received 17 August 2005; accepted 21 January 2006; published online 28 February 2006)

Direct numerical simulation (DNS) and large-eddy simulation (LES) of particle-laden turbulent channel flow, in which the particles experience a drag force, are investigated for two subgrid models and several Reynolds and Stokes numbers. In this flow, turbophoresis leads to an accumulation of particles near the walls. The objectives of the work are to investigate the accuracy of the subgrid models studied with respect to particle behavior and to explain the observed particle behavior predicted by the different models. The focus is on particle dispersion and mean particle motion in the direction normal to the walls of the channel. For a low Reynolds number, it is shown that the turbophoresis and particle velocity fluctuations are reduced compared to DNS, if the filtered fluid velocity calculated in the LES is used in the particle equation of motion. This is a combined effect of the disregard of the subgrid scales in the fluid velocity and the inadequacy of the subgrid model. Better agreement with DNS is obtained if an inverse filtering model, which was recently proposed, is incorporated into the particle equation. This model is shown to enhance turbophoresis and particle velocity fluctuations in actual LES. The results of the approximate deconvolution model (ADM) agree better with DNS results than results of the dynamic eddy-viscosity model. This can be explained from the better prediction of the fluid velocity statistics by ADM and the better correspondence of the subgrid models adopted in the fluid and particle equations. Although the differences between the two subgrid models become smaller, similar conclusions are obtained at a higher Reynolds number. Compared to fourth-order interpolation of the fluid velocity to the particle position, second-order interpolation approximately cancels the effect of the subgrid model in the particle equation of motion. © *2006 American Institute of Physics*. [DOI: 10.1063/1.2176589]

I. INTRODUCTION

In many examples in industry and the environment, particles are transported in a turbulent flow. The motion of the particles is affected by the fluid flow; for example, by a drag force and lift force. If the particles are small compared to the smallest length scales of the fluid flow, a point-particle description can be employed.[1,2] The fluid is then modeled as a continuous phase, while for each particle an equation of motion is imposed. Direct numerical simulations (DNS) of particle-laden turbulent flows in simple geometries, such as pipe flow and channel flow, have been carried out in this way.[3–5]

For single-phase flows, large-eddy simulation (LES) has gradually become a more and more powerful tool, which produces acceptable results with much less computational effort compared to DNS. The development of more accurate subgrid modeling strategies, such as dynamic modeling,[6] approximate deconvolution models,[7] the variational multiscale model,[8,9] and the regularization principle,[10] have demonstrated the large potential of LES for various single-phase turbulent flows.

In the last decade, LES has also been applied to particle-laden flows. The particle equation of motion always contains the fluid velocity, and in an LES only the resolved part of the fluid velocity is known. In many examples, the equation of motion for the particles is solved with the filtered fluid velocity[5,11,12] without incorporating a model for the subgrid scales. When the particle relaxation time is large compared to the Kolmogorov time scale and the smallest time scale resolved in the LES, this approach is justified.[5] Armenio *et al.*[13] studied the effects of the disregard of the subgrid scales in the particle equation of motion by *a priori* and *a posteriori* simulation of particle-laden channel flow, but they restricted to quantities and test cases where the effect of the subgrid scales is small.

In contrast, in Refs. 14 and 15 it has been shown that a phenomenon as turbophoresis, where particles move towards the walls of a channel by the effect of the turbulence, cannot accurately be predicted if the subgrid scales in the fluid velocity are disregarded in the particle equation of motion. The results depend on the subgrid model applied, but even for an "optimal" subgrid model, a substantial difference between the DNS and LES results remains, especially for particle relaxation times of the same order as the Kolmogorov time. It has also been shown[14,15] that results improve if a defiltered fluid velocity[16] is used in the particle equation of motion, and if an adequate subgrid model, such as the dynamic eddy-viscosity model,[6] is applied. Later, a similar deconvolution model was proposed as a subgrid model in the particle equation by Shotorban and Mashayek,[17] who applied this procedure in LES of particle-laden homogeneous shear flow.

The defiltering procedure proposed in Ref. 14 remains somewhat arbitrary, since the filter adopted has no relation to

[a)]Electronic mail: j.g.m.kuerten@tue.nl

the filter applied in the LES. In contrast, in the approximate deconvolution model (ADM),[7] an explicit inverse filter is used in the LES itself. Application of the deconvolved velocity to both the fluid and particle equations would yield a more uniform method. Therefore, in this article it will be studied whether the deconvolved fluid velocity of the ADM can also be used in the particle equation of motion. In order to compare results, LES of particle-laden turbulent channel flow will be carried out for two different subgrid models: the dynamic eddy-viscosity model[6] and ADM.[7] Simulations will be performed with and without the defiltering procedure. Results will be compared with DNS results on a fine grid, on which all relevant length scales are resolved, and on a coarse LES grid, which serves as an LES without a subgrid model.

Simulations will be performed at two Reynolds numbers: a low Reynolds number ($\mathrm{Re}_\tau=150$), and a higher Reynolds number ($\mathrm{Re}_\tau=590$), for which no DNS results of particle-laden flow are available. Particles with three different particle relaxation times will be studied, which lie around the average Kolmogorov time of the flow. Particles with the same time scale as the fluid are most influenced by the turbulence. Quantities that will be investigated are mean particle velocity, particle velocity fluctuation, and particle concentration.

The article is organized as follows. In the next section, the equations of motion and numerical methods for particles and fluid are formulated. In Sec. III results are shown and explained for DNS and LES, including results obtained with the defiltering procedure. Finally, in Sec. IV conclusions are stated and discussed.

II. GOVERNING EQUATIONS AND NUMERICAL METHOD

In this section the equations of motion and numerical methods for fluid and particles are described. Moreover, the defiltering procedure is elucidated.

A. Fluid

The flow considered in this article is incompressible turbulent channel flow. The Navier-Stokes equation is solved in rotation form:[18]

$$\frac{\partial \mathbf{u}}{\partial t} + \omega \times \mathbf{u} + \nabla P = \nu \Delta \mathbf{u} + \mathbf{F}, \tag{1}$$

where $\omega=\nabla\times\mathbf{u}$ is the vorticity, $P=p/\rho_f+\frac{1}{2}\mathbf{u}^2$, ν is the fluid kinematic viscosity, p the fluctuating part of the pressure, and ρ_f is the fluid density. Finally, $\mathbf{F}$ is the driving force, chosen constant in time and space. In that way, the time-averaged Reynolds number based on the friction velocity u_τ ($\mathrm{Re}_\tau=Hu_\tau/\nu$) can be specified, where H is half the channel height.

In the DNS all relevant length scales and time scales are resolved. In the streamwise and spanwise directions, periodic boundary conditions are applied. Therefore, the use of a pseudospectral method is very convenient. In the two periodic directions, a Fourier-Galerkin approach is applied, whereas a Chebyshev-collocation method is adopted in the wall-normal direction.

The time integration is performed with a combination of the second-order-accurate implicit Crank-Nicolson method for the viscous and pressure terms and a third-order-accurate compact-storage explicit Runge-Kutta method for the other terms. This makes the total method second-order accurate. The nonlinear term is calculated by transforming from Fourier space to real space and back with fast Fourier transform. In order to prevent aliasing errors, the 3/2-rule is applied in the periodic directions. The velocity field is made divergence free within machine accuracy following the approach proposed by Kleiser and Schumann[19] applied to the collocation approximation.[18]

The computational domain has a size $2H$ in the wall-normal direction, $4\pi H$ in streamwise direction, and $2\pi H$ in spanwise direction. In the DNS ($\mathrm{Re}_\tau=150$), the number of Chebyshev collocation points equals 129 and 128 Fourier modes are used in both periodic directions. This makes the dimensions of the channel in wall units equal to 300 in the wall-normal direction, 1885 in the streamwise direction, and 942 in the spanwise direction. Moreover, $\Delta x^+=14.7$, $\Delta z^+=7.4$, and Δy^+ ranges between 0.045 at the walls and 3.7 at the center of the channel. Throughout the article, x, y, and z are used for streamwise, wall-normal, and spanwise directions, respectively. The simulation was started from Poiseuille flow, onto which several of the least stable two- and three-dimensional disturbances according to linear stability theory were superposed. Due to nonlinear interactions, transition to turbulence occurs and after a large number of time steps, a state of fully developed turbulence appears.

In the LES calculations an equation for a spatially filtered fluid velocity $\bar{\mathbf{u}}$ is solved, where

$$\bar{\mathbf{u}}(\mathbf{x}) = \int_V G(\mathbf{x};\mathbf{y})\mathbf{u}(\mathbf{y})d^3y. \tag{2}$$

The integral extends over the whole domain and $G(\mathbf{x};\mathbf{y})$ is a filter function; e.g., the top-filter or a spectral cutoff filter. Filtering of the Navier-Stokes equation for the fluid velocity leads to the turbulent stress tensor $\tau_{i,j}$ given by

$$\tau_{ij} = \overline{u_i u_j} - \bar{u}_i \bar{u}_j, \tag{3}$$

which depends on the unfiltered fluid velocity and hence is unknown in a LES. Here, it is assumed that the filter operator commutates with all derivatives and that the viscosity is constant. Otherwise, more subgrid terms appear in the filtered Navier-Stokes equation. In a large-eddy simulation the turbulent stress tensor is replaced by a subgrid model, which is expressed in terms of the known filtered fluid velocity.

In this work, two subgrid models are considered: the dynamic eddy-viscosity model,[6] which is based on Smagorinsky's eddy-viscosity model,[20] and the approximate deconvolution model (ADM).[7] Moreover, for comparison purposes, calculations on a coarse LES grid without subgrid model are performed. In the dynamic eddy-viscosity model

$$\tau_{ij} = -C_d\Delta^2|S(\bar{\mathbf{u}})|S_{ij}(\bar{\mathbf{u}}), \tag{4}$$

where S_{ij} is the rate of strain tensor given by

$$S_{ij}(\mathbf{u}) = \frac{\partial u_i}{\partial x_j} + \frac{\partial u_j}{\partial x_i}$$

and $|S(\mathbf{u})| = \frac{1}{2} S_{ij}(\mathbf{u}) S_{ij}(\mathbf{u})$. Furthermore, Δ is the typical width of the filter. In the present application of channel flow, the filter width in each direction is taken equal to the grid size, and

$$\Delta = (\Delta_x \Delta_y \Delta_z)^{1/3}$$

is taken as the typical filter width, which depends on the wall-normal coordinate. Finally, the coefficient C_d is dynamically adjusted to the local structure of the flow. The coefficient is determined by the introduction of a test filter with filter width 2Δ and application of the Germano identity.[6] Following Lilly,[21] the dynamic coefficient is averaged over the homogeneous directions. As a test filter, the top-hat filter is applied.

The basis of ADM is replacement of the unfiltered velocity in τ_{ij} by an approximate deconvolution of the filtered velocity, according to

$$\tau_{ij} = \overline{u_i^* u_j^*} - \bar{u}_i \bar{u}_j, \tag{5}$$

where

$$u_i^* = Q_N \bar{u}_i = \sum_{k=0}^{N} (I - G)^k \bar{u}_i \tag{6}$$

and G is the filter kernel. The filter and the implementation of the model are the same as in the original paper by Stolz *et al.*[7] In this work, the choice of $N=5$ is made as well. In order to represent the effects of the subgrid scales, an extra regularization term is added to the Navier-Stokes equation:

$$\frac{\partial \bar{\mathbf{u}}}{\partial t} + \overline{\omega^* \times \mathbf{u}^*} + \nabla \bar{P} = \nu \Delta \bar{\mathbf{u}} + \mathbf{F} - \chi (I - Q_N G) \bar{u}, \tag{7}$$

where χ is dynamically adjusted in such a way that the kinetic energy contained in the smallest resolved scales remains constant in time.[7]

The numerical method used for the LES is the same as for the DNS. The turbulent stress tensor is treated in the same way as the other nonlinear terms in the Navier-Stokes equation. For the ADM, de-aliasing is also performed in the wall-normal direction. Simulations at two Reynolds numbers are performed. The low Reynolds case ($\mathrm{Re}_\tau = 150$), for which DNS is also performed, uses 33 Chebyshev collocation points in the wall-normal direction, 32 Fourier modes in the streamwise direction, and 64 in the spanwise direction. Since the computational domain is the same as in the corresponding DNS ($\Delta x^+ \approx 59$ and $\Delta z^+ \approx 15$), which satisfies the requirements of a resolved LES (for details, see Piomelli and Balaras[22]). This resolution corresponds to $\Delta / h_{\mathrm{DNS}} = 4$ in the wall-normal and streamwise directions, and to $\Delta / h_{\mathrm{DNS}} = 2$ in the spanwise direction. The LES simulations are started from filtered DNS fields. After some time, a statistically stationary LES solution is obtained.

In addition, simulations at a higher Reynolds number ($\mathrm{Re}_\tau = 590$) are performed for the dynamic eddy-viscosity model and ADM. In these simulations, the computational domain has a size $2H$ in the wall-normal direction, $2\pi H$ in the streamwise direction, and πH in the spanwise direction. The resolution is 65 Chebyshev points in the wall-normal direction, 48 Fourier modes in the streamwise direction, and 96 in the spanwise direction. As $\Delta x^+ \approx 77$ and $\Delta z^+ \approx 19$, the requirements of a resolved LES are satisfied as well. At this Reynolds number, no particle-laden DNS was performed due to the high computational requirements, but some results can be compared to the DNS without particles at the same Reynolds number by Moser *et al.*[23] The test cases performed are summarized in Table I. Herein, Re_m, the Reynolds number based on the mean velocity, is also included. For the low Reynolds number case, we see that the mean velocity is overpredicted compared to the DNS results for both subgrid models, whereas the mean velocity of the coarse grid DNS is underpredicted. Of the subgrid models studied, ADM agrees best with the DNS. At the high Reynolds number, where according to the results by Moser *et al.*[23] $\mathrm{Re}_m = 10\,935$, the agreement in mean velocity is better and again ADM is slightly more accurate than the dynamic model.

TABLE I. Parameters of the numerical simulations performed.

Case	Model	Grid	Domain	Re_τ	Re_m
DNS-150	None	$128 \times 129 \times 128$	$4\pi \times 2 \times 2\pi$	150	2 290
Dyn-150	Dynamic	$32 \times 33 \times 64$	$4\pi \times 2 \times 2\pi$	150	2 400
ADM-150	ADM	$32 \times 33 \times 64$	$4\pi \times 2 \times 2\pi$	150	2 380
Nomodel-150	None	$32 \times 33 \times 64$	$4\pi \times 2 \times 2\pi$	150	2 170
Dyn-590	Dynamic	$48 \times 65 \times 96$	$2\pi \times 2 \times \pi$	590	11 160
ADM-590	ADM	$48 \times 65 \times 96$	$2\pi \times 2 \times \pi$	590	10 990

B. Particles

Particles are described by an equation of motion for each particle. In the present work only the drag force will be considered, which has been justified by Armenio *et al.*[24] Particle-particle interaction and the effect of particles on the fluid will be disregarded. This is justified for the low particle concentrations considered in this article. Hence, the equation of motion for a particle i with instantaneous position $\mathbf{x}_i$, velocity $\mathbf{v}_i$, and mass m_i reads[1]

$$\frac{d\mathbf{v}_i}{dt} = \frac{\mathbf{u}(\mathbf{x}_i, t) - \mathbf{v}_i}{\tau_p} (1 + 0.15 \mathrm{Re}_p^{0.687}), \tag{8}$$

where $\mathbf{u}(\mathbf{x}_i, t)$ is the fluid velocity at the position of the particle. The particle relaxation time τ_p quantifies the drag by the fluid on the particle and is given by $\tau_p = \rho_p d_p^2 / (18 \rho_f \nu)$, where d_p is the particle diameter. The standard drag correlation for particles with particle Reynolds number Re_p is not small compared to 1 is applied.[25]

In the low Reynolds number simulations shown here, $\rho_p / \rho_f = 769.23$, and three different diameters are investigated: $d_{p,1}/H = 1.02 \times 10^{-3}$, $d_{p,2}/H = 2.28 \times 10^{-3}$, and $d_{p,3}/H = 5.10 \times 10^{-3}$. This corresponds to Stokes numbers, defined as $\mathrm{St} = \tau_p^+ = \tau_p u_\tau^2 / \nu$, of 1, 5, and 25. In Fig. 1(a), the Kolmogorov time of the DNS and the typical subgrid time scales of the LES models have been plotted as a function of the wall-normal coordinate. The subgrid time scale is inversely pro-

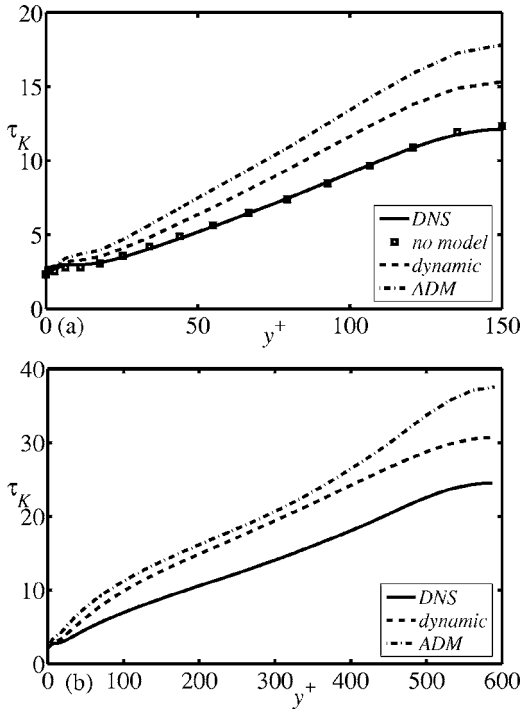

FIG. 1. Kolmogorov time and typical subgrid time scales for (a) $\mathrm{Re}_\tau=150$ and (b) $\mathrm{Re}_\tau=590$.

portional to the square root of the resolved dissipation rate. The lowest particle relaxation time studied is lower than the smallest turbulent time scale throughout the channel. Hence, these particles are affected by all time scales present in the flow; to disregard the subgrid scales will influence the particle behavior in the whole channel. The highest particle relaxation time studied is larger than the smallest time scale of the flow, both in the DNS and in the LES. This implies that the effect of disregarding the subgrid scales in the fluid velocity will not influence the results much, since these scales hardly affect the particles in this case. Particles with $\mathrm{St}=5$, on the other hand, have a particle relaxation time equal to the channel-averaged Kolmogorov time. Especially around $y^+=25$, the Kolmogorov time is close to the particle relaxation time, and the effect of the disregard of the subgrid scales in the fluid velocity will be appreciable. This is exactly the region where the turbophoretic velocity, which leads to particle accumulation at the walls, is largest. The difference between the two LES results in this figure shows that the small scales, which contribute more to the energy dissipation rate than to the kinetic energy, are smaller in ADM than in the dynamic model.

In the $\mathrm{Re}_\tau=590$ simulations, particles with the same mass density and the same three Stokes numbers are investigated. These Stokes numbers yield different particle diameters than at the lower Reynolds number, given by $d_{p,1}/H=2.64\times10^{-4}$, $d_{p,2}/H=5.90\times10^{-4}$, and $d_{p,3}/H=1.32\times10^{-3}$. The typical time scale at this Reynolds number is shown in Fig. 1(b), where results from the DNS by Moser *et al.*[23] are also included. It can be seen that the three particles relaxation times investigated at this Reynolds number are comparable to the ones studied at $\mathrm{Re}_\tau=150$: the lowest is smaller and the largest is larger than the typical time scale of the flow throughout the channel, whereas the intermediate Stokes number is equal to the Kolmogorov time in the region where the turbophoretic velocity is largest.

In the particle-laden simulations, (8) is solved with the second-order-accurate Heun method. In order to find the fluid velocity at the particle position, an interpolation has to be made. In this work, in the two periodic directions fourth-order Lagrange interpolation,[26] and in the wall-normal direction, fourth-order Hermite interpolation is applied. The particle-laden simulations start from a statistically stationary state of fully-developed turbulence with 100 000 particles of each Stokes number randomly distributed uniformly over the channel. A particle collides elastically with the walls when it reaches one of the walls within a distance equal to its radius. If a particle leaves the computational domain through one of the periodic boundaries, its position is still tracked and the fluid velocity at the particle position follows from periodic continuation of the velocity field.

Solution of (8) gives accurate results in DNS, but in the particle-laden LES simulations the fluid velocity present in (8) is unknown and simulations with the fluid velocity replaced by the filtered fluid velocity result in substantial deviations in statistical particle quantities compared to DNS. It is, however, possible to decrease the subgrid errors in the LES results by retrieving part of the subgrid contributions to the fluid velocity by inverse filtering. Inverse filtering frequently occurs in the literature of LES,[7,16,27] where it is used to model the turbulent stress tensor. It has often been successful provided that a dissipation term is added to control the extra fluctuations introduced by defiltering. Recently, Kuerten and Vreman[14,15] and later Shotorban and Maskayek[17] showed that defiltering of the fluid velocity also yields a useful subgrid model in the particle equation of motion.

In the present work, the defiltering depends on the subgrid model and is carried out in the following way. In the dynamic eddy-viscosity model a filter only appears explicitly as test filter. Assuming that the primary filter has the same shape, we adopt the top-hat filter with filter width Δ as the primary filter. The inversion is performed in Fourier space in the two periodic directions, whereas in the wall-normal direction the inverse is approximated with a Taylor series up to second order in the filter width. (Note that this corresponds to $N=1$ in the approximate deconvolution proposed by Shotorban and Mashayek,[17] who applied a Gaussian filter.) At the walls the defiltered velocity is set equal to zero. In the ADM simulations the deconvolved velocity field $\mathbf{u}^*$, defined in (6), is used with $N=5$, just as in the filtered Navier-Stokes equation.

III. RESULTS

In this section, results of the particle simulations are presented. In the first subsection, results at the low Reynolds number ($\mathrm{Re}_\tau=150$) are presented and DNS results are compared with the results of both subgrid models with and without the subgrid model in the particle equation of motion. In the second subsection results at the higher Reynolds number

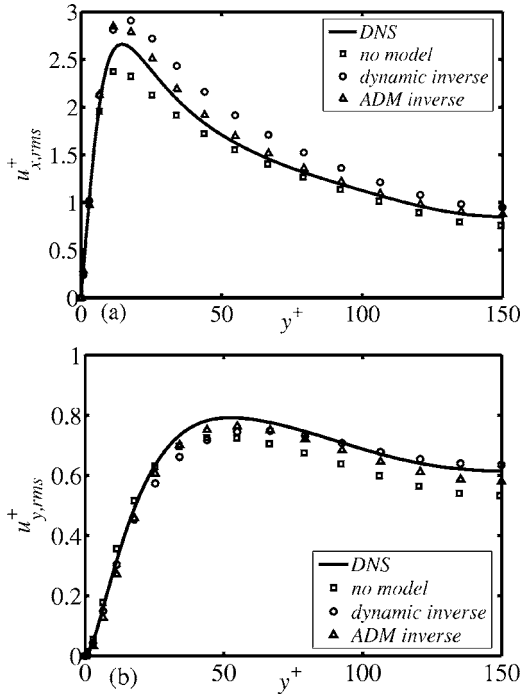

FIG. 2. Fluid velocity fluctuations for $\mathrm{Re}_\tau=150$: (a) streamwise component and (b) wall-normal component.

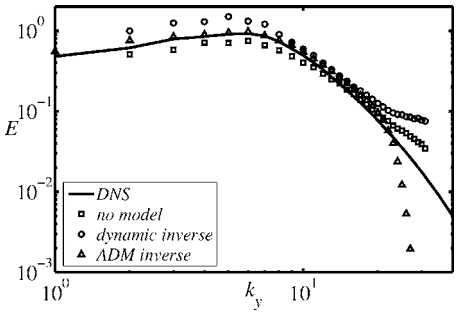

FIG. 3. Spanwise one-dimensional energy spectrum of the fluid at $y^+=25$ and $\mathrm{Re}_\tau=150$.

are discussed and, where possible, compared with the DNS results of single-phase fluid flow by Moser *et al.*[23]

A. $\mathrm{Re}_\tau=150$

DNS results will be compared with LES results for both subgrid models, both with the filtered and with the defiltered fluid velocity adopted in (8). Results without subgrid model are also included. A good subgrid model should yield results better than without subgrid model. The discussion will be restricted to three quantities: mean particle velocity, particle concentration, and particle velocity fluctuations. The latter quantity determines particle dispersion, whereas the other two are directly related to the phenomenon of turbophoresis. First, however, some results of the fluid properties are shown, which are important to interpret the particle results.

1. Fluid properties

The streamwise and the wall-normal fluid velocity fluctuations, which have a large influence on the particle behavior, are shown in Fig. 2 as a function of the wall-normal coordinate for $\mathrm{Re}_\tau=150$. As the DNS results cannot directly be compared with the LES results, the LES results are based on the defiltered fluid velocity. For the streamwise velocity fluctuations, the ADM results agree much better with the DNS results than the dynamic model results. The too-large streamwise velocity fluctuations are a well-known drawback of the dynamic eddy-viscosity model, and this is even enhanced by the defiltering. The LES without subgrid model yields lower streamwise velocity fluctuations than the DNS, in particular near the maximum. The wall-normal velocity fluctuations of the dynamic model agree better with the DNS, but ADM yields slightly better results throughout the height of the channel. Finally, it can be observed that the wall-normal velocity fluctuations calculated without subgrid model are quite good close to the walls, but too low in the central part of the channel. The results of both components indicate that ADM is better capable of predicting the anisotropic properties of channel flow than the dynamic model, whereas the LES without subgrid model is clearly more inaccurate than both subgrid models.

In order to better understand the results presented in the following section, the one-dimensional kinetic energy spectrum in spanwise direction at $y^+=25$ is shown in Fig. 3, zoomed in on the region of highest importance. This result shows that the spectrum obtained with defiltered ADM corresponds very well with the DNS result for wave numbers smaller than 20. At higher wave numbers the ADM spectrum decreases very quickly, corresponding to the high-order filter applied in this model and this is only partly canceled by defiltering. The results of the defiltered dynamic model do not show this decrease at high wave numbers and yield a too-high energy for wave numbers larger than 20. The too-high kinetic energy at lower wave numbers is solely due to the streamwise velocity component, which has too-high fluctuations in this model, as noted in Fig. 2. Finally, it can be seen that the results without subgrid model distribute the energy over the wave numbers in the wrong way: due to the absence of subgrid dissipation, the energy contained in the smallest waves is too high, and this is at the expense of the energy contained in the lower wave numbers. As shown in Fig. 1(a), however, the total energy dissipation rate corresponds very well with the DNS result.

2. Mean wall-normal particle velocity

Although the mean wall-normal fluid velocity component equals zero, the mean wall-normal particle velocity is initially unequal to zero. This phenomenon is called turbophoresis and leads to the accumulation of particles near the walls, which has been measured[28] and numerically predicted in DNS of turbulent channel and pipe flow.[3,4] This particle transport mechanism is caused by the inhomogeneity of the turbulent velocity fluctuations[29,30] and can be understood mathematically from the following perturbation expansion of (8) in case the particle relaxation time is small.

We search for a solution of the form $\mathbf{v}=\mathbf{v}^{(0)}+\tau_p\mathbf{v}^{(1)}+\cdots$, substitute this in (8), and gather terms with the same power of τ_p. This yields in lowest order

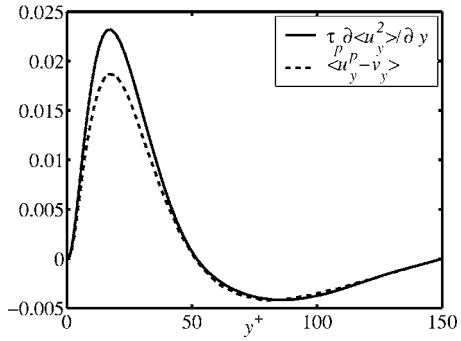

FIG. 4. Mean relative velocity at St=1 and Re_τ=150.

$$\mathbf{v}^{(0)}(\mathbf{x},t) = \mathbf{u}(\mathbf{x}(t),t), \tag{9}$$

which implies that a particle moves with the local fluid velocity, which is of course the limiting situation for passive particles with zero relaxation time. Substitution of this solution in the equation for the next order in τ_p results in

$$\mathbf{v}^{(1)} = -\frac{\partial \mathbf{u}}{\partial t} - \mathbf{u} \cdot \nabla \mathbf{u}, \tag{10}$$

where it is understood that the fluid velocity is evaluated at the particle position. To find the average wall-normal particle velocity, the two terms for v are added and averaged over all particles at a certain wall-normal coordinate. The result is

$$\langle v_y \rangle = \langle u_y^p \rangle - \tau_p \frac{\partial}{\partial y} \langle u_y^2 \rangle + \cdots, \tag{11}$$

where $\mathbf{u}^p$ is the fluid velocity at the particle position.

Initially, when the particles are homogeneously distributed, $\langle u_y^p \rangle = 0$ and $\langle v_y \rangle$ will be directed towards the walls. After a long time, a statistically stationary particle concentration will be reached, in which $\langle v_y \rangle = 0$. Equation (11) shows that the particles are then preferentially located at positions where the instantaneous fluid velocity is directed away from the wall. The validity of (11) at small Stokes number is shown in Fig. 4, where $\langle u_y^p - v_y \rangle$ and $\tau_p \partial / \partial y \langle u_y^2 \rangle$ are shown for the DNS at St=1 as functions of the wall-normal coordinate. As $\tau_p u_{\mathrm{rms}}/H \simeq 1$ is not really small, the agreement is not perfect, but quite good.

In Fig. 5 the mean relative velocity is shown for all simulations and the three particle relaxation times. All results have been averaged over time until $t^+ = 16\,000$ and over the two homogeneous directions. Equation (11) indicates that the relative velocity is independent of time, and this indeed appears from the numerical results, apart from a small initial transient. In order to show the differences between the different models more clearly, the figures are restricted to the most interesting region close to the wall. A first observation from these figures is that for all three Stokes numbers, the LES results without defiltering underpredict the maximum in the relative velocity. This can be explained from (11) and Fig. 2. According to (11), the relative velocity is caused by the inhomogeneity of the wall-normal velocity fluctuations. Both subgrid models result in decreased velocity fluctuations and hence in a smaller relative velocity. The relative difference between the DNS and LES results is larger at the two

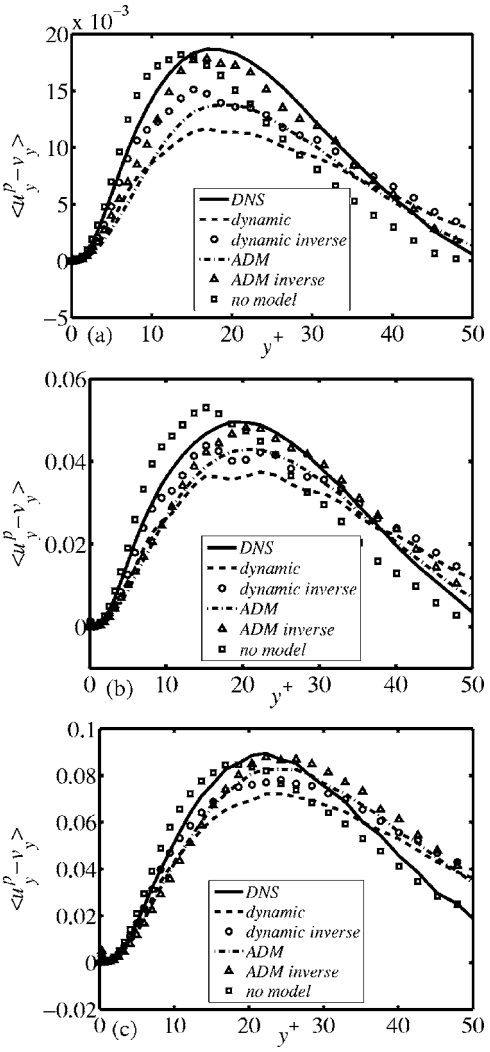

FIG. 5. Mean relative velocity at Re_τ=150 and (a) St=1, (b) St=5 and (c) St=25.

lower Stokes numbers, where the effect of the small scales in the fluid velocity on the particle motion is largest. Moreover, it can be seen that ADM agrees better with the DNS than the dynamic eddy-viscosity model.

A second observation is that defiltering improves the LES results. This results in only small differences between DNS and defiltered ADM results. The results of the dynamic model are less accurate, especially at the lowest Stokes number where the effect of the turbulence on the particles is largest. Apparently, the agreement between the subgrid models used in the filtered Navier-Stokes equation and the particle equation of motion is beneficial for an accurate prediction of particle behavior. The relative effect of defiltering is smaller at the largest Stokes number, which can also be explained from the fact that these largest particles respond less to the smaller scales of the velocity fluctuations, which are most enhanced by the defiltering.

A final observation is that the results without subgrid modeling are, for this relative particle velocity, almost as accurate as ADM with defiltering. This can also be explained from the agreement of the wall-normal velocity fluctuations with the DNS in the near-wall region shown in Fig. 2. How-

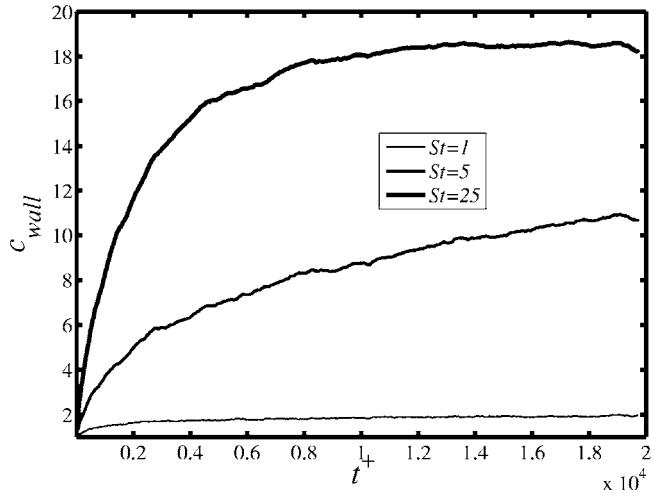

FIG. 6. Concentration of particles close to the wall as a function of time calculated by DNS.

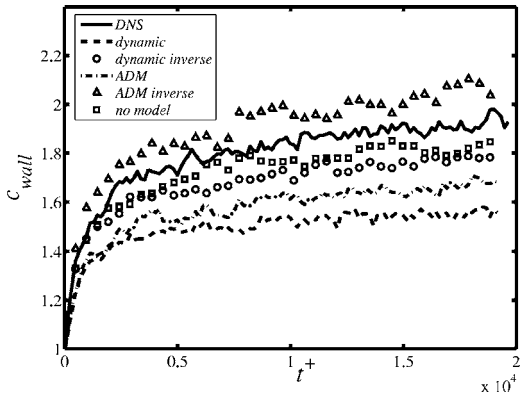

FIG. 7. Concentration of particles close to the wall as a function of time for $Re_\tau=150$ and St=1.

ever, the good agreement does by no means imply that subgrid modeling is not necessary. First, several single-phase results are not accurately predicted without subgrid model, as shown in Figs. 2 and 3. Second, not all particle statistical quantities correspond as well with DNS results, as will be shown later. Finally, simulations at higher Reynolds number tend to become unstable if no subgrid model is adopted.

3. Particle concentration

The nonzero mean wall-normal particle velocity leads to accumulation of particles near the walls of the channel. In Fig. 6 the concentration of particles close to the walls is plotted as a function of time for the DNS calculations at the three Stokes numbers. To this end, the computational domain is divided in 40 equidistant strips parallel to the walls and particles in the strips closest to both walls are counted. The particle concentration is normalized in such a way that for a uniform distribution, $c=1$. The effect of turbophoresis is clearly visible. The concentration close to the walls increases as a function of time: first fast, and later, due to the nonuniformity of particle distribution, more slowly until a statistically stationary particle concentration is reached. The particle concentration close to the walls increases with increasing Stokes number in the regime investigated. The stationary particle concentration is reached at the latest time for the middle Stokes number: St=5. It has been shown by *a priori* analysis by Kuerten and Vreman[14] that turbophoresis is reduced when the fluid velocity in (8) is filtered and that this effect is largest when the particle relaxation time is equal to the Kolmogorov time. For these particles, the effect of the turbulence on their motion is largest.

In Fig. 7, the results for St=1 are gathered for all models studied. As for the mean relative velocity, the results of both subgrid models without defiltering underpredict the particle accumulation and again ADM is somewhat better. For ADM and the dynamic model the results with defiltering show a significant improvement. Finally, the results without subgrid model are as accurate as the defiltered ADM and dynamic model and also agree quite well with the DNS results. Again, this follows from the fact that this coarse grid DNS yields almost the same wall-normal velocity fluctuations as the unfiltered DNS. Similar results are obtained at the other two Stokes numbers.

In Fig. 8 the mean particle concentration in the stationary state is plotted as a function of the wall-normal coordinate. It is averaged over time from $t^+=16\,000$ to $t^+=20\,000$ and over the homogeneous directions. The results are similar as for mean relative wall-normal velocity: defiltering of the fluid velocity gives significant improvement, of the subgrid models studied defiltered ADM gives the best agreement with DNS, but for this quantity the performance of the coarse grid DNS is as accurate. Moreover, the effect of defiltering decreases at larger Stokes numbers.

4. Particle velocity fluctuations

Particle dispersion is directly influenced by the particle velocity fluctuations. In Fig. 9, the streamwise particle velocity fluctuations have been plotted for St=1, averaged over time from $t^+=1000$ to $t^+=16\,000$ and over the homogeneous directions. In addition, this quantity does not depend on time, apart from a small initial transient. The streamwise particle velocity fluctuations are slightly larger than the fluid velocity fluctuations. This cannot be understood from a first-order perturbation expansion in the Stokes number as performed above to explain the mean relative wall-normal velocity. It turns out that the first-order term equals approximately zero and a higher-order expansion involves moments of the velocity up to fourth order, which are difficult to assess numerically.

Since the dynamic model overpredicts the streamwise fluid velocity fluctuations, it is not surprising that the particle velocity fluctuations are also overpredicted by this model. Defiltering only deteriorates this result, since it increases the fluid velocity fluctuations felt by the particles. On the other hand, the defiltered ADM results agree quite well with the DNS results. Finally, the increase in particle velocity fluctuations compared to the fluid velocity fluctuations is not observed in the results without subgrid model. Hence, the difference between this result and DNS is increased with

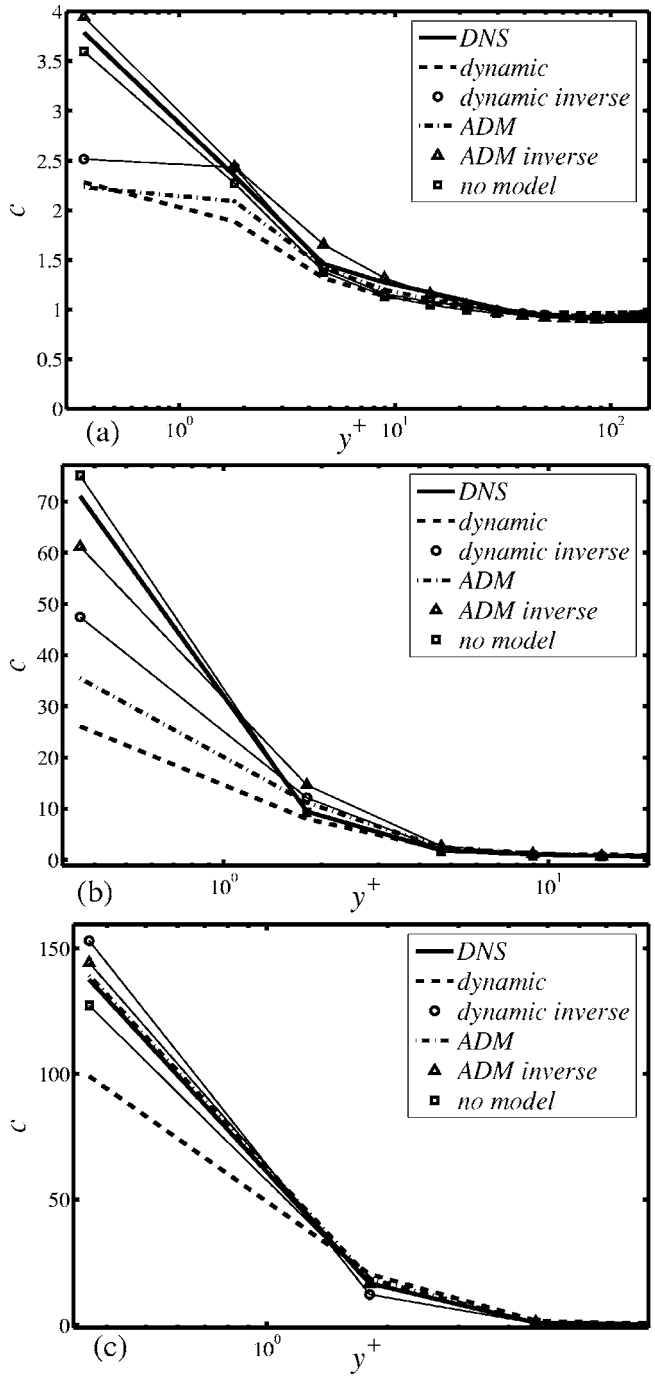

FIG. 8. Concentration of particles in the stationary state for $\mathrm{Re}_\tau=150$ and (a) $St=1$, (b) St=5, and (c) St=25.

respect to the fluid velocity fluctuations. The explanation for this observation can be found in the too-low kinetic energy contained in the low wave numbers.

Similar results are obtained for the streamwise particle velocity fluctuations at the other Stokes numbers. In all cases, the defiltered ADM results slightly overpredict the peak value, but agree best with the DNS results. The peak value of the streamwise particle velocity fluctuations increases from St=1 to St=5 and slightly to St=25, whereas the velocity fluctuations decrease mildly with increasing Stokes number near the center of the channel.

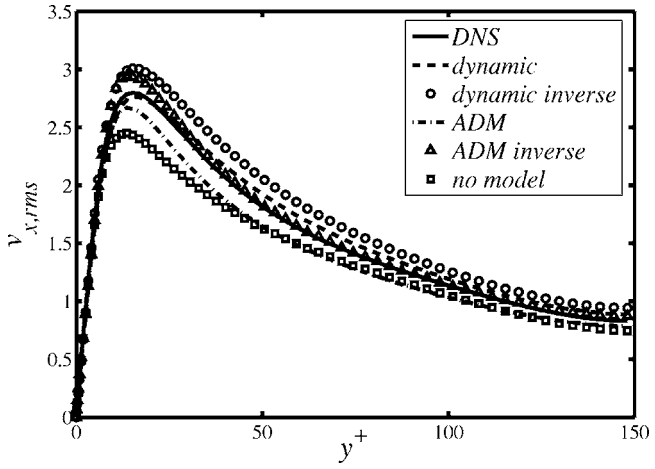

FIG. 9. Streamwise particle velocity fluctuations at St=1 and $\mathrm{Re}_\tau=150$.

In Fig. 10, the wall-normal particle velocity fluctuations have been plotted for the three Stokes numbers. The figure shows the well-known result that the wall-normal particle velocity fluctuations are smaller than their fluid counterparts, and decrease for increasing Stokes number. A similar perturbation analysis in the Stokes number as above shows that

$$\langle v_y^2\rangle = \langle u_y^2\rangle - 2\tau_p \frac{d}{dy}\langle u_y^3\rangle + \cdots, \tag{12}$$

which involves the skewness of the wall-normal fluid velocity. Since $d\langle u_y^3\rangle/dy$ is positive in the whole channel apart from a very small region adjacent to the walls, with a value of approximately 0.01 for $y^+\approx 25$, the behavior of the wall-normal particle velocity fluctuations can be understood both qualitatively and quantitatively. Both subgrid models, similar to the fluid results shown in Fig. 2, yield smaller particle velocity fluctuations than the DNS, but defiltering improves the results. The defiltered ADM results show the best agreement with DNS. Especially for St=5 and St=25 the difference between defiltered ADM and DNS is small. The results without subgrid model are clearly less accurate. This is a combined effect of the too small fluid velocity fluctuations and the more inaccurate prediction of the skewness of the wall-normal fluid velocity. The two subgrid models studied also do not predict the wall-normal skewness accurately, but defiltering improves the prediction.

Finally in Fig. 11, the spanwise particle velocity fluctuations are shown for St=1. For this quantity the defiltered dynamic model is almost as good as defiltered ADM and both models agree well with the DNS. Close to the wall the results without subgrid model are as good as the defiltered results of the two models, but near the center of the channel the LES without subgrid model produces too-low spanwise velocity fluctuations. Similar results are obtained for the higher Stokes numbers.

As a conclusion, it can be stated that at this Reynolds number the defiltered ADM gives the best results. The defiltered dynamic model has as main disadvantage that the streamwise velocity fluctuations are too high, which is typical for an isotropic eddy-viscosity model. In general, the spanwise and wall-normal velocity components are better

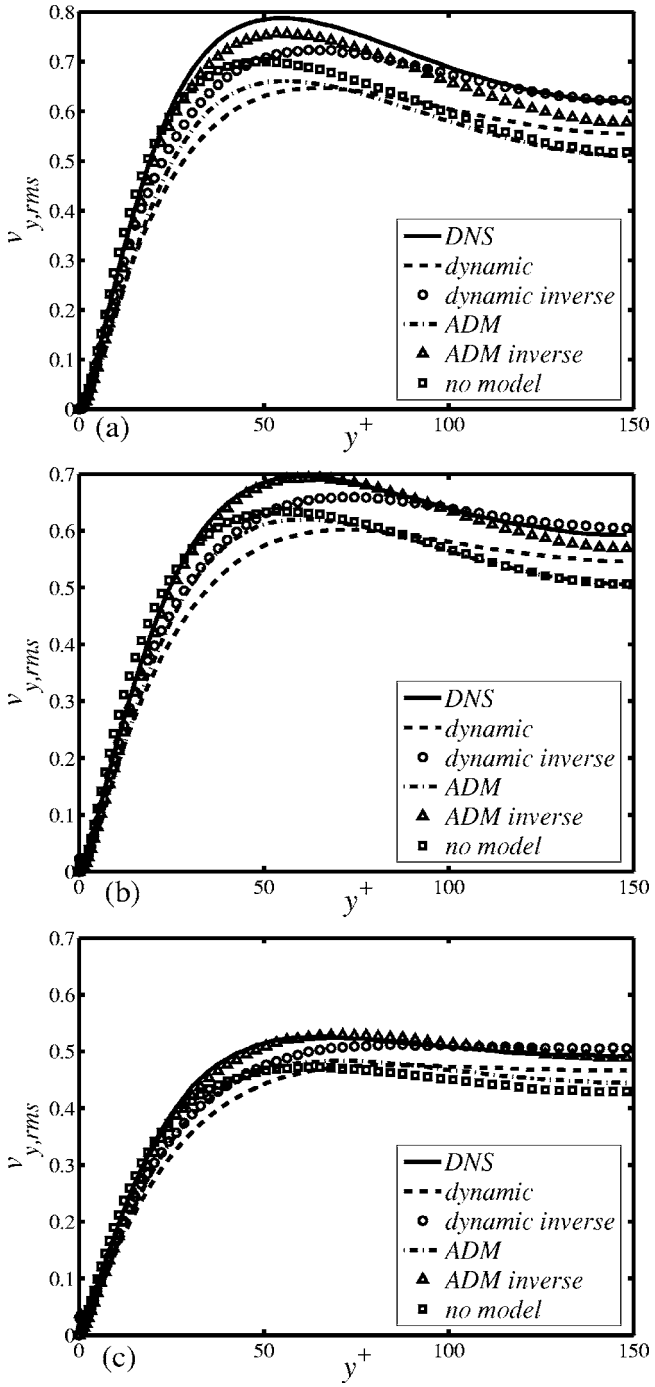

FIG. 10. Wall-normal particle velocity fluctuations at $Re_\tau=150$ and (a) St =1, (b) St=5, and (c) St=25.

predicted. For first moments of particle velocity the LES without subgrid model also yields good results, but its prediction of particle (and fluid) velocity fluctuations is not accurate. Moreover, LES without subgrid model becomes unstable at higher Reynolds numbers. Therefore, in the next subsection only the dynamic model and ADM will be studied at a higher Reynolds number.

B. $Re_\tau=590$

As mentioned in the previous section, it is more difficult to assess the accuracy of the results at the higher Reynolds number, since there are no results available of particle-laden DNS at this Reynolds number. However, the fluid DNS of Moser *et al.*[23] is available and some of the particle statistics at low Stokes number is almost equal to the fluid statistics. For instance, the particle velocity fluctuations at St=1 should be approximately equal to the fluid velocity fluctuations, as we also saw for the low Reynolds number in the previous subsection. Hence, this subsection is intended to show that the defiltering also works at a higher Reynolds number, to study the effect of defiltering at this Reynolds number and to compare, where possible, particle results at low Stokes number with fluid results calculated with DNS.

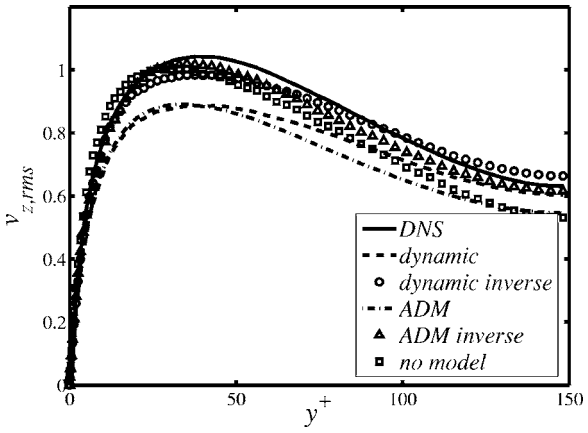

FIG. 11. Spanwise particle velocity fluctuations at St=1 and $Re_\tau=150$.

1. Fluid properties

As at the lower Reynolds number, first results for the fluid are compared. In Fig. 12, the streamwise and wall-normal defiltered fluid velocity fluctuations are compared

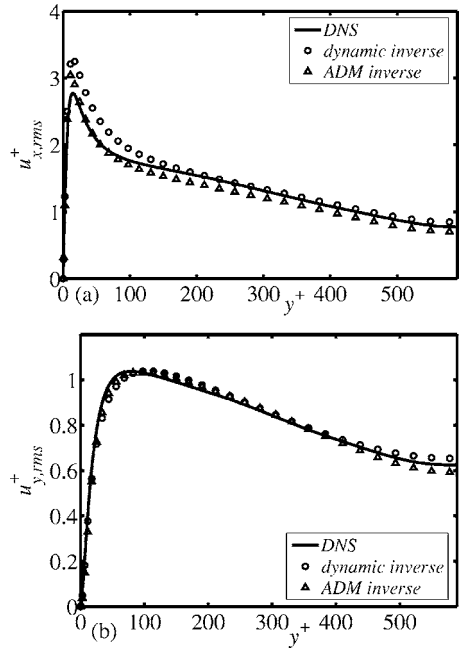

FIG. 12. Fluid velocity fluctuations for $Re_\tau=590$: (a) streamwise component and (b) wall-normal component.

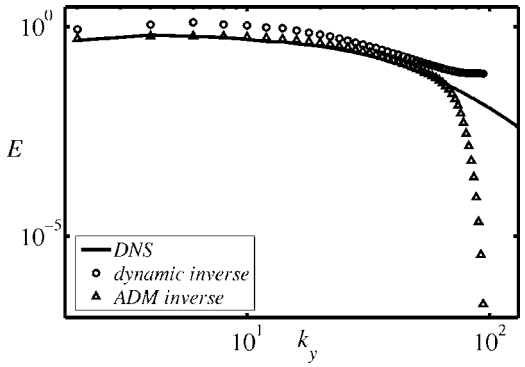

FIG. 13. Spanwise one-dimensional energy spectrum of the fluid at $y^+=30$ and $\mathrm{Re}_\tau=590$.

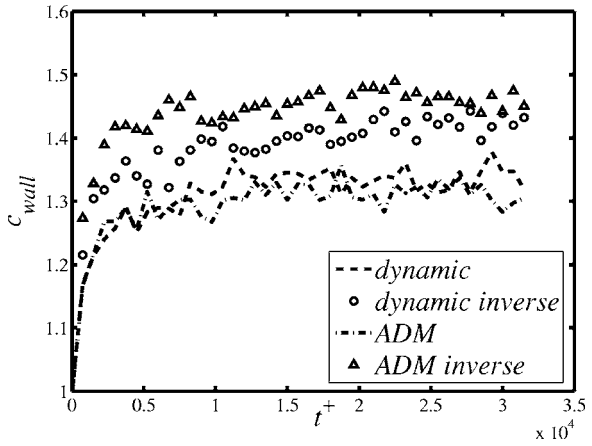

FIG. 15. Concentration of particles close to the wall as a function of time for St=1 and $\mathrm{Re}_\tau=590$.

with results by Moser *et al.* In addition, at this Reynolds number the streamwise fluid velocity fluctuations predicted by the defiltered dynamic model are too high, and the ADM results are clearly better. The wall-normal defiltered fluid velocity fluctuations agree quite well with the DNS for both models with defiltered ADM slightly better near the walls. For the one-dimensional kinetic energy spectrum in the spanwise direction, which is shown at $y^+=30$ in Fig. 13, similar conclusions follow as in the low Reynolds number case: the dynamic model yields a too-high energy spectrum for all wave numbers, which is at low wave numbers caused by the too-high streamwise velocity fluctuations and at high wave numbers by insufficient damping. Defiltered ADM agrees very well with the DNS results apart from the tail of the spectrum, which is too low for wave numbers larger than 70.

2. Mean wall-normal particle velocity

As a first particle result, the mean relative velocity at St=1 is shown in Fig. 14. Included is the DNS result for $\tau_p \partial / \partial y \langle u_y^2 \rangle$, which, according to (11), should agree for values of the particle relaxation time small compared to the Lagrangian time scale of the flow. As also at this Reynolds number this condition is not satisfied for $St=1$, exact agreement cannot be expected. However, if a similar difference between the right-hand side and left-hand side of (11) is assumed as at $\mathrm{Re}_\tau=150$, it appears that again ADM performs better than the dynamic model and that defiltering improves the results of both models.

3. Particle concentration

As a next result, the wall concentration is plotted as a function of time for St=1 in Fig. 15. As for the lower Reynolds number, particles accumulate in the near-wall region and a statistically stationary state is reached at $t^+ \approx 16\,000$. The increase in particle concentration near the wall is less than at $\mathrm{Re}_\tau=150$. In contrast to $\mathrm{Re}_\tau=150$, the results of the two subgrid models are almost equal, as is the effect of defiltering. At the two higher Stokes numbers, the defiltered ADM results in a lower wall concentration than the defiltered dynamic model.

4. Particle velocity fluctuations

As a final result, the particle velocity fluctuations are studied. In Fig. 16, the streamwise velocity fluctuations are shown for St=1. Included are the streamwise fluid velocity fluctuations taken from the DNS of Moser *et al.*,[23] which should be almost equal to the particle velocity fluctuations at

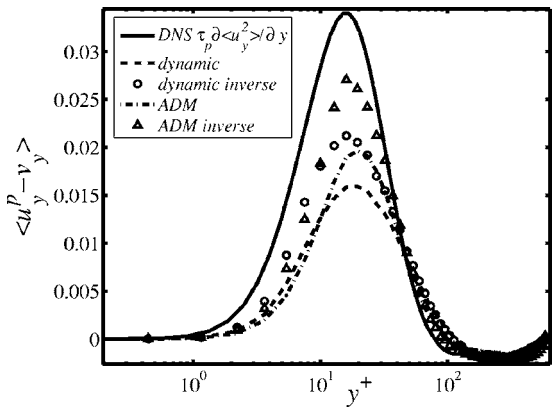

FIG. 14. Mean relative velocity at St=1 and $\mathrm{Re}_\tau=590$.

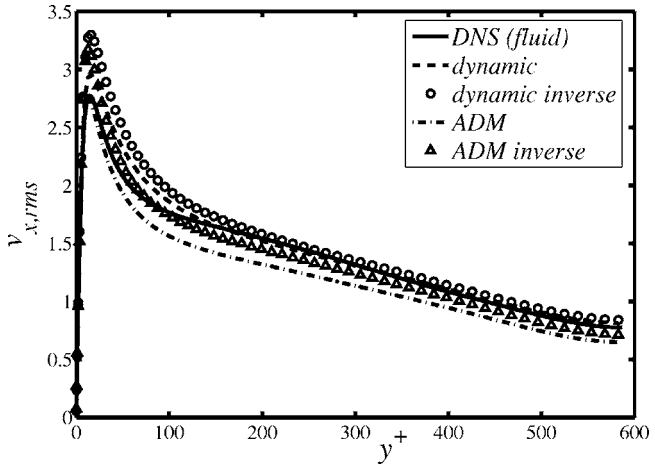

FIG. 16. Streamwise particle velocity fluctuations at St=1 and $\mathrm{Re}_\tau=590$.

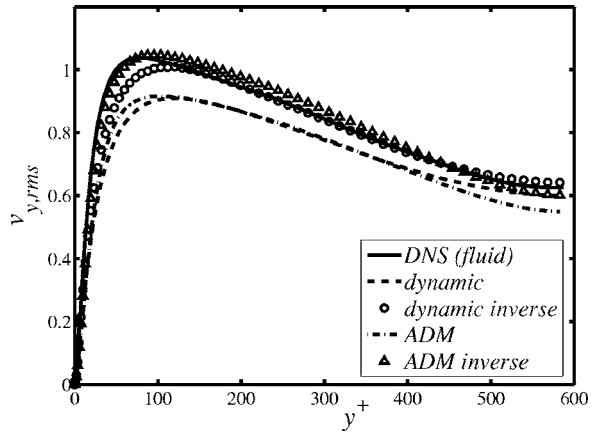

FIG. 17. Wall-normal particle velocity fluctuations at St=1 and Re_τ=590.

this low Stokes number. The too-large value of the peak compared to the fluid velocity fluctuation is similar as at the lower Reynolds number. The difference between the results of the two subgrid models is also the same as at the lower Reynolds number. As at Re_τ=150, the streamwise fluid velocity fluctuations of the dynamic model at this Reynolds number are larger than the DNS result.

The fluctuations of the two other velocity components are shown in Figs. 17 and 18 for the St=1 case. For both components, the defiltered ADM agrees well with the DNS results and the defiltered dynamic model performs worse, especially for the wall-normal component, but better than at the lower Re_τ. Moreover, the effect of defiltering is appreciable. A more quantitative comparison, based on (12), can be made for the wall-normal velocity fluctuations. The DNS results of Moser *et al.*[23] show that at this Reynolds number the first-order term in τ_p in (12) is negligible. Hence, at this Stokes number, the particle velocity fluctuations should coincide with the fluid velocity fluctuations. Therefore, Fig. 17 shows that defiltered ADM gives better results than the defiltered dynamic model. It turns out that this is caused by the difference in particle velocity fluctuations and fluid velocity fluctuations in the dynamic model and not by the defiltered fluid velocity fluctuations predicted by this model, which correspond quite well with the DNS. Indeed, the skewness of

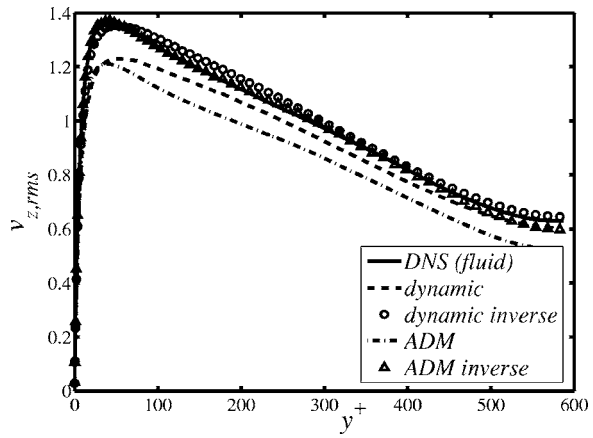

FIG. 18. Spanwise particle velocity fluctuations at St=1 and Re_τ=590.

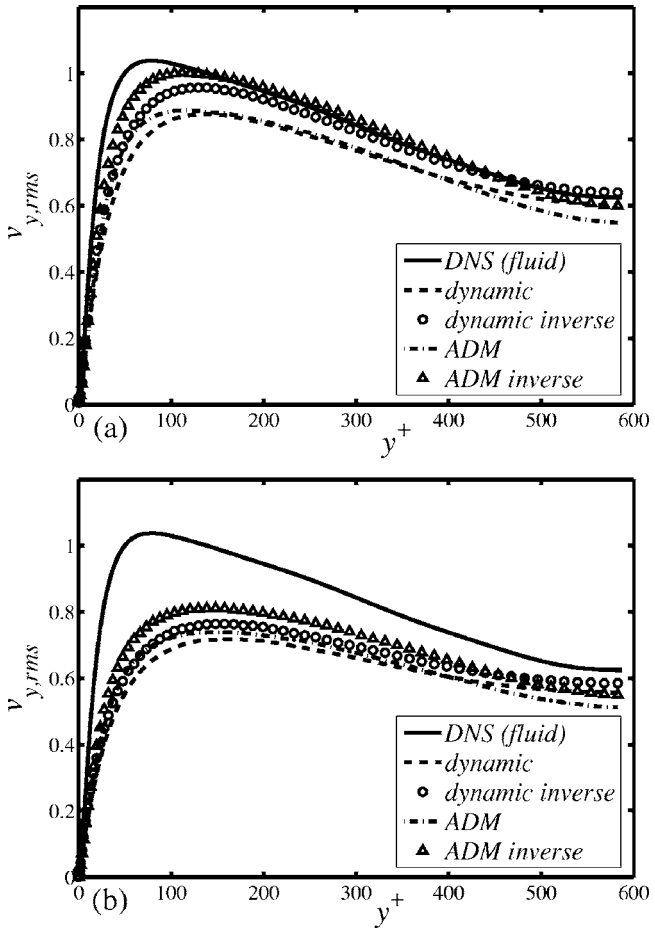

FIG. 19. Wall-normal particle velocity fluctuations at Re_τ=590 and (a) St=5 and (b) St=25.

the wall-normal fluid velocity predicted by the dynamic model is larger than that predicted by ADM [see (12)].

To see the effect of different Stokes number, the wall-normal velocity fluctuations are plotted for St=5 and St=25 in Fig. 19. The DNS result is included again, but as the wall-normal velocity fluctuations decrease for increasing Stokes number, this serves only for comparison purposes. The LES results both decrease for increasing Stokes number as they should. Moreover, the effect of defiltering decreases at larger Stokes numbers. This is in agreement with the result shown in Fig. 1(b), that the particle relaxation time is larger than the Kolmogorov time throughout the channel, so that the subgrid scales of the fluid velocity affect the particle motion less.

IV. DISCUSSION AND CONCLUSIONS

In this article, LES of particle-laden turbulent channel flow is studied for two subgrid models, at three different Stokes numbers and two Reynolds numbers. In order to model the subgrid effects in the particle equation of motion the fluid velocity is deconvolved with the use of an approximate inverse of the filter. The objective of this work is twofold: first, to investigate which subgrid model performs best and second, to understand the particle behavior observed—specifically, particle dispersion and wall-normal particle ve-

locity. To this end, DNS and LES without subgrid model are also performed for the lower Reynolds number case.

The subgrid model in the particle equation of motion significantly improves the results for both subgrid models, and its effect is largest at the two lower particle relaxation times studied, where particles are most influenced by the small scales of the fluid velocity. Of the two subgrid models studied, the approximate deconvolution model agrees best with the DNS results. The results of the dynamic eddy-viscosity model are less accurate—in particular, the mean wall-normal particle velocity and the streamwise particle velocity fluctuations deviate from the DNS results. An important reason is that this isotropic eddy-viscosity model is not capable of accurately predicting the fluid velocity fluctuations in regions where the flow is anisotropic. Moreover, from a theoretical point of view ADM has the advantageous property that the same defiltering operation is used in the subgrid model for the fluid and in the subgrid model for the particles. It turns out that this also results in better agreement with DNS. Although for some particle properties the results of LES without subgrid model are as accurate as the defiltered ADM results or even slightly better, the absence of a subgrid model in the Navier-Stokes equation is not an option, since several flow properties, in particular the velocity fluctuations of fluid and particles, are too inaccurate. Besides, LES without subgrid model suffers from stability problems at higher Reynolds numbers.

Apart from the results shown, results have also been calculated with the Smagorinsky subgrid model, which is still often used in commercial computational fluid dynamics simulations. For all quantities considered, the results were far less accurate than those obtained with the other models and defiltering did not show much improvement.

In all results shown, fourth-order-accurate interpolation has been applied to obtain the fluid velocity at the particle position. Simulations with second-order (trilinear) interpolation have also been performed for the dynamic eddy-viscosity model. It appears that this results in substantially smaller particle concentrations near the wall and velocity fluctuations. For both quantities, the second-order results with defiltering closely resemble the fourth-order results without defiltering. This can be understood from the fact that compared to fourth-order interpolation, second-order interpolation acts as an additional filter, thus largely canceling the action of the defiltering operator. It has been shown that the interpolation error is very small if fourth-order interpolation is applied.[31]

The two subgrid models were also tested at a higher Reynolds number. Since no particle-laden DNS results were available, only a few results, notably at a small Stokes number, could be compared with DNS. In general, defiltered ADM provides the best results, but the differences between the two subgrid models are smaller than at the lower Reynolds number. Again, the effects of defiltering were quite large at the lower two Stokes numbers.

The results shown in this article clearly indicate that the proposed subgrid model in the particle equation of motion yields a substantial improvement. An advantage of this subgrid model is that it is very easy to implement, both in spectral methods and in finite volume methods. In the simulations presented the computing time needed for the inversion was only approximately 3% of the time needed for the velocity interpolation. Moreover, the same subgrid model can be applied in case two-way or four-way coupling is applied and if other forces between fluid and particles, such as lift force, added mass and pressure drag, are taken into account. For the latter two forces also the fluid acceleration should be defiltered and for the lift force the fluid vorticity, but that can be done in exactly the same way.

Defiltering only models the effects of the resolved scales, in sofar they are affected by the filtering operator. Subgrid scales, which are not represented on the LES grid, cannot be retrieved by deconvolution. This article shows that in general the subgrid scales hardly affect statistical properties of particle motion, such as mean particle concentration and mean and root-mean-square of particle velocity. This can be explained by the fact that the subgrid scales are less coherent than the larger scales of the fluid velocity and hence only influence instantaneous particle behavior. In statistical particle properties these effects cancel.

ACKNOWLEDGMENTS

This work was sponsored by the Stichting Nationale Computerfaciliteiten (National Computing Facilities Foundation, NCF) for the use of supercomputer facilities, with financial support from the Nederlandse Organisatie voor Wetenschappelijk Onderzoek (Netherlands Organization for Scientific Research, NWO). The author is grateful to Dr. A. W. Vreman for many discussions on this topic and to Dr. S. Stolz for providing information on ADM.

[1] M. R. Maxey and J. J. Riley, "Equation of motion for a small rigid sphere in a nonuniform flow," Phys. Fluids **26**, 883 (1983).
[2] M. Boivin, O. Simonin, and K. D. Squires, "On the prediction of gas-solid flows with two-way coupling using large-eddy simulation," Phys. Fluids **12**, 2080 (2000).
[3] C. Marchioli and A. Soldati, "Mechanisms for particle transfer and segregation in a turbulent boundary layer," J. Fluid Mech. **468**, 283 (2002).
[4] C. Marchioli, A. Giusti, M. V. Salvetti, and A. Soldati, "Direct numerical simulation of particle wall transfer and deposition in upward turbulent pipe flow," Int. J. Multiphase Flow **29**, 1017 (2003).
[5] W. S. J. Uijttewaal and R. V. A. Oliemans, "Particle dispersion and deposition in direct numerical and large eddy simulation of vertical pipe flows," Phys. Fluids **8**, 2590 (1996).
[6] M. Germano, U. Piomelli, P. Moin, and W. H. Cabot, "A dynamic subgrid-scale eddy viscosity model," Phys. Fluids A **3**, 1760 (1991).
[7] S. Stolz, N. A. Adams, and L. Kleiser, "An approximate deconvolution model for large-eddy simulation with application to incompressible wall-bounded flows," Phys. Fluids **13**, 997 (2001).
[8] T. J. R. Hughes, A. A. Oberai, and L. Mazzei, "Large eddy simulation of turbulent channel flows by the variational multiscale method," Phys. Fluids **13**, 1784 (2001).
[9] A. W. Vreman, "The filtering analog of the variational multiscale method in large-eddy simulation," Phys. Fluids **15**, L61 (2003).
[10] B. J. Geurts and D. D. Holm, "Regularization modeling for large-eddy simulation," Phys. Fluids **15**, L13 (2003).
[11] F. Yeh and U. Lei, "On the motion of small particles in a homogeneous isotropic turbulent flow," Phys. Fluids A **3**, 2571 (1991).
[12] Q. Wang and K. D. Squires, "Large eddy simulation of particle deposition in a vertical turbulent channel flow," Int. J. Multiphase Flow **22**, 667 (1996).
[13] V. Armenio, U. Piomelli, and V. Fiorotto, "Effect of the subgrid scales on particle motion," Phys. Fluids **11**, 3030 (1999).

[14] J. G. M. Kuerten and A. W. Vreman, "Can turbophoresis be predicted by large-eddy simulation?" Phys. Fluids **17**, 011701 (2005).
[15] J. G. M. Kuerten, "A subgrid model for large-eddy simulation of particle-laden channel flow," in Proceedings of the 11th Workshop on Two-Phase Flow Predictions, edited by M. Sommerfeld, 2005, ISBN 3-96010-767-4.
[16] J. G. M. Kuerten, B. J. Geurts, A. W. Vreman, and M. Germano, "Dynamic inverse modelling and its testing in LES of the mixing layer," Phys. Fluids **11**, 3778 (1999).
[17] B. Shotorban and F. Mashayek, "Modeling subgrid-scale effects on particles by approximate deconvolution," Phys. Fluids **17**, 081701 (2005).
[18] C. Canuto, M. Y. Hussaini, A. Quarteroni, and T. A. Zang, *Spectral Methods in Fluid Dynamics* (Springer, Berlin, 1988).
[19] L. Kleiser and U. Schumann, "Treatment of incompressibility and boundary conditions in 3-D numerical spectral simulations of plane channel flows," in *Proceedings of the Third GAMM-Conference on Numerical Methods in Fluid Mechanics*, edited by E. H. Hirschel (Vieweg, Braunschweig, 1980), pp. 165–173.
[20] J. Smagorinsky, "General circulation experiments with the primitive equations," Mon. Weather Rev. **91**, 99 (1963).
[21] D. K. Lilly, "A proposed modification of the Germano subgrid-scale closure method," Phys. Fluids A **4**, 633 (1992).
[22] U. Piomelli and E. Balaras, "Wall-layer models for large-eddy simulations," Annu. Rev. Fluid Mech. **34**, 349 (2002).
[23] R. D. Moser, J. Kim, and N. N. Mansour, "Direct numerical simulation of turbulent channel flow up to Re_τ=590," Phys. Fluids **11**, 943 (1999).
[24] V. Armenio and V. Fiorotto, "The importance of the forces acting on particles in turbulent flows," Phys. Fluids **13**, 2437 (2001).
[25] R. Clift, J. R. Grace, and M. E. Weber, *Bubble, Drops and Particles* (Academic, Boston, 1978).
[26] S. Balachandar and M. R. Maxey, "Methods for evaluating fluid velocities in spectral simulations of turbulence," J. Comput. Phys. **83**, 96 (1989).
[27] B. J. Geurts, "Inverse modeling for large-eddy simulation," Phys. Fluids **9**, 3585 (1997).
[28] B. Y. H. Liu and J. K. Agarwal, "Experimental observation of aerosol deposition in turbulent flow," J. Aerosol Sci. **5**, 145 (1974).
[29] M. W. Reeks, "The transport of discrete particles in inhomogeneous turbulence," J. Aerosol Sci. **14**, 729 (1983).
[30] J. Young and A. Leeming, "A theory of particle deposition in turbulent pipe flow," J. Fluid Mech. **340**, 129 (1997).
[31] J. G. M. Kuerten, "A priori testing of large-eddy simulation of particle-laden channel flow," in Proceedings of the 3rd International Symposium on Two-Phase Flow Modelling and Experimentation, Pisa, 2004.